Outage Performance of Exponentiated Weibull FSO Links Under Generalized Pointing Errors

Rubén Boluda-Ruiz, Antonio García-Zambrana,
Carmen Castillo-Vázquez, Beatriz Castillo-Vázquez and Steve Hranilovic

***Abstract*—Even in clear conditions, free-space optical (FSO) links are impaired by scintillation and dynamic misalignment which result in a slow fading channel. This paper presents the first characterization of outage performance for single-input/single-output (SISO) FSO links over exponentiated Weibull (EW) atmospheric turbulence and generalized misalignment. A novel feature of this paper is that a generalized pointing error model is employed which not only takes into account the impact of different jitters for the elevation and the horizontal displacement but also the effect of different boresight errors for each axis. The developed asymptotic expressions are used to find optimum beam widths that minimize the impact of pointing error effects in a variety of atmospheric turbulence conditions. Obtained results corroborate that the impact of generalized pointing errors is approximately the same over moderate and strong turbulence conditions when an aperture-averaged receiver is considered. Additionally, the use of a transmitter with optimized beam width can result in large gains on the order of 5 dB or even greater.**

***Index Terms*—Free-space optical (FSO), outage probability (OP), pointing errors and outage diversity (O_d).**

I. Introduction

FREE-SPACE optical (FSO) systems offer a number of advantages including a license-free spectrum, immunity to radio-frequency (RF) interferences as well as robustness to eavesdropping [1]. However, such communication systems are vulnerable to both atmospheric turbulence and pointing error effects even in clear weather, which can greatly reduce its performance. Atmospheric turbulence results in fluctuations in both the intensity and the phase of the received optical beam, severely degrading the link performance. Pointing error effects at the receiver produced by wind loads and thermal expansions result in building sways leading to a misalignment between transmitter and receiver. In this paper, for the first time, we characterize the outage probability in the case of both atmospheric turbulence with generalized pointing errors with independent boresight errors and jitter variances. The expressions serve as a design tool to optimize outage performance through proper beam width selection in FSO links.

A large number of statistical models have been proposed to model the impact of turbulence-induced scintillation in FSO systems. Log-normal (LN) distributions are accurate in weak turbulence conditions, Gamma-Gamma (GG) distributions are accurate for moderate-to-strong atmospheric turbulence and exponential distributions are appropriate in very strong turbluence [2]. A challenge in these statistical models is that they often do not provide a good fit to simulation data in the moderate-to-strong turbulence regime where the impact of aperture averaging can be significant [3]. Recently, an exponentiated Weibull (EW) model was proposed, which provides a good fit between simulation and experimental data under moderate-to-strong aperture averaging conditions [4]–[7]. This atmospheric turbulence model has been used in a significant number of research articles [8]–[16] in order to study the performance of FSO communication systems.

Similarly, the statistical modeling of misalignment in FSO systems is critical to characterize communication performance [17]–[20]. In [17], a pointing error model was proposed where effect of beam width, detector size and independent identical distributed (iid) Gaussian distributions for the elevation and the horizontal displacement were considered. This work was extended to consider different jitter variances in elevation and the horizontal displacement [18] and by considering nonzero boresight error at the receiver for iid Gaussian jitter distributions [19]. In [20], a generalized pointing error model was considered with different jitters for the elevation and the horizontal displacement as well as the nonzero boresight errors to compute ergodic capacity for FSO links over LN and GG fading channels. In recent years, the combined impact of EW fading and pointing errors has been studied in different FSO scenarios [10], [12]–[15]. In [10], the ergodic capacity is studied over EW atmospheric turbulence with zero boresight pointing errors. In [12], closed-form expressions for the outage probability and the bit error rate (BER) were obtained for various binary modulation schemes over EW atmospheric turbulence with pointing errors. In [13], a multi-hop FSO communication systems with decode-and-forward (DF) relay transmission over the EW fading channels with pointing errors was proposed. In [14] a closed-form expression for the outage capacity was derived in terms of the H-Fox function over EW atmospheric turbulence with nonzero boresight pointing errors. Furthermore, expressions obtained in [5, eqs. (20)-(22)] for the EW parameters have been used recently in [15] in order to investigate the asymptotic ergodic capacity of multiple-input/multiple-output (MIMO) FSO systems under different aperture averaging conditions and nonzero boresight pointing errors. It should be highlighted that a generalized pointing errors model was not used in any research papers mentioned

Rubén Boluda-Ruiz, Antonio García-Zambrana and Beatriz Castillo-Vázquez are with the Department of Communications Engineering, University of Málaga, Málaga, Spain (e-mail: rbr@ic.uma.es, agz@ic.uma.es, bcv@ic.uma.es).

Carmen Castillo-Vázquez is with the Department of Mathematical Analysis, Statistics and Operations Research and Applied Mathematics, University of Málaga, Málaga, Spain (e-mail: carmelina@uma.es).

Steve Hranilovic is with the Department of Electrical and Computer Engineering, McMaster University, Ontario, Canada (e-mail: hranilovic@mcmaster.ca).

above.

This paper focuses on the asymptotic outage performance of FSO links over EW atmospheric channels with generalized pointing errors following a Beckmann distribution [21] by using a moment generating function (MGF)-based approach. It must be noted that there are no published papers that investigate the outage performance of FSO systems over EW atmospheric turbulence with generalized pointing errors taking into account the effect of aperture averaging. Unlike [18], [19], a generalized pointing error model is taken into account here, wherein not only the effect of different jitters for the elevation and the horizontal displacement is carefully analyzed but also the simultaneous effect of different boresight errors for each axis is studied. Also, unlike [20], where a generalized pointing error model was also considered for studying the ergodic capacity, the outage probability of EW FSO links is adopted here as a more suitable metric performance for FSO systems than ergodic capacity due to the fact that atmospheric turbulence is well described as slow fading. Moreover, the impact of generalized pointing errors on FSO communication systems is analyzed in-depth and minimized according to an optimum beam width for terrestrial FSO applications by using the derived asymptotic expressions for the outage probability. Simulation results are further included to confirm the analytical results.

The remainder of the paper is organized as follows. System and channel models are described in Sections II and III, respectively. In Section IV, we obtain the asymptotic closed-form expression for the outage probability by using an MGF-based approach, wherein generalized pointing errors follow a Beckmann distribution. This asymptotic closed-form expression is totally valid for most practical FSO systems. Numerical results and discussions are presented in Section V as well as some interesting conclusions are commented on Section VI.

II. System Model

Consider a single-input/single-output (SISO) FSO communications link using on-off keying (OOK) modulation. The use of infrared technologies based on intensity-modulation and direct-detection (IM/DD) is assumed here due to their simplicity and low cost. The intensity of the emitted light is used to transmit the information, and the photodetector directly detects changes in the light intensity without the need for a local oscillator. The received electrical signal for a SISO FSO link is given by

$$y = hRx + z, \tag{1}$$

where R is the detector responsivity, assumed hereinafter to be the unity, x is the transmitted optical power, h is the equivalent real-value fading gain of the channel between the source and the receiver, and z is additive white Gaussian noise (AWGN) with zero mean and variance $\sigma^2 = N_0/2$. The channel gain is a product of three factors, i.e. $h = L \cdot h_a \cdot h_p$, atmospheric path loss L, atmospheric turbulence h_a, and geometric spread and pointing errors h_p. Note that both atmospheric turbulence and pointing errors are considered to be statistically independent. The path loss, L, is determined by the exponential Beers-Lambert law as $L = e^{-\Phi d_{SD}}$, where d_{SD} is the link distance and Φ is the atmospheric attenuation coefficient described in [22]. The received electrical signal-to-noise ratio (SNR) can be defined as $\gamma_T = 4\gamma h^2$, where $\gamma = P_{\text{opt}}^2 T_b/N_0$ represents the normalized received electrical SNR in absence of turbulence, P_{opt} is the average transmitted optical power and T_b is the bit period.

III. Channel Model

Atmospheric turbulence is modeled using the EW distribution in order to consider a wide range of turbulence conditions (weak-to-strong) as well as aperture averaging conditions i.e., when the condition $D \geq \rho_0$ holds, where D represents the diameter of a circular detection aperture ($D = 2a$) and $\rho_0 = 0.79\left(C_n^2 \kappa^2 d_{SD}\right)^{-3/5}$ is the plane wave coherence radius [2]. Here, $\kappa = 2\pi/\lambda$ is the optical wave number, and C_n^2 is the refractive index structure parameter. The corresponding probability density function (PDF) was derived in [4, eqn. (7)] as follows

$$\begin{aligned} f_{h_a}(h_a) =& \frac{\alpha\beta}{\eta}\left(\frac{h_a}{\eta}\right)^{\beta-1} \exp\left[-\left(\frac{h_a}{\eta}\right)^{\beta}\right] \\ &\times \left\{1 - \exp\left[-\left(\frac{h_a}{\eta}\right)^{\beta}\right]\right\}^{\alpha-1}, \quad h_a \geq 0 \end{aligned} \tag{2}$$

where $\beta > 0$ is a shape parameter related to the scintillation index (SI), $\eta > 0$ is a scale parameter related to the mean value of the irradiance and $\alpha > 0$ is an extra shape parameter that is strongly dependent on the receiver aperture size. By fitting the EW turbulence model to simulated or experimental PDF data, several specific values of the parameters α, β and η as well as some expressions for evaluating these parameters have been obtained in [4], [5]. In this paper, expressions obtained in [5, eqs. (20)-(22)] are used for moderate-to-strong turbulence conditions. The expressions corresponding to the EW parameters are given as a function of the scintillation index, σ_I^2, as follows

$$\alpha = \frac{7.220\sigma_I^{2/3}}{\Gamma\left(2.487\sigma_I^{2/6}\right) - 0.104}, \tag{3a}$$

$$\beta = 1.012(\alpha\sigma_I^2)^{-13/25} + 0.142, \tag{3b}$$

$$\eta = \frac{1}{\alpha\Gamma\left(1 + 1/\beta\right) g_1(\alpha,\beta)}, \tag{3c}$$

where $g_1(\alpha,\beta)$ is defined as follows

$$g_1(\alpha,\beta) = \sum_{k=0}^{\infty} \frac{(-1)^k \Gamma(\alpha)}{k!(k+1)^{1+1/\beta}\Gamma(\alpha-k)}. \tag{4}$$

It must be noted that expressions obtained in [5, eqs. (20)-(22)] are valid when the aperture averaging (AA) $AA < 0.9$ [5]. The aperture averaging factor, AA, can be defined by the normalized variance of power fluctuations of the incident optical field on a collecting lens. It can also be defined by the ratio of the irradiance flux variance obtained by a finite-size collecting lens to that obtained by a point-like receiver [23], i.e. $AA = \sigma_I^2(D)/\sigma_I^2(0)$, where $\sigma_I^2(D)$ and $\sigma_I^2(0)$ denote the scintillation indexes for a receive aperture of diameter D and a point-like receiver, respectively. The scintillation index is

expressed as in [2, eqn. (69), Chapter 10] under both weak and strong turbulence conditions as follows

$$\sigma_I^2(D) = \exp\left(\frac{0.49\sigma_R^2}{\left(1+0.65d^2+1.11\sigma_R^{12/5}\right)^{7/6}}\right) \times \exp\left(\frac{0.51\sigma_R^2\left(1+0.69\sigma_R^{12/5}\right)^{-(5/6)}}{1+0.9d^2+0.62d^2\sigma_R^{12/5}}\right) - 1, \tag{5}$$

where the parameter d is defined as $d = \sqrt{\kappa D^2/4d_{SD}}$. The scintillation index, $\sigma_I^2(D)$, can also be expressed as a function of the EW parameters [5, eqn. (19)].

The attenuation due to geometric spread and pointing errors can be approximated, as in [17, eqn. (9)], as follows

$$h_p(r;z) \approx A_0 \exp\left(\frac{-2r^2}{\omega_{z_{eq}}^2}\right), \tag{6}$$

where $v = \sqrt{\pi}a/\sqrt{2}\omega_z$, $A_0 = [\text{erf}(v)]^2$ is the fraction of the collected power at $r = 0$, and $\omega_{z_{eq}}^2 = \omega_z^2\sqrt{\pi}\text{erf}(v)/2v\exp(-v^2)$ is the equivalent beam width. The radial displacement r at the receiver plane can be expressed as $r^2 = x^2 + y^2$, where x and y represent the horizontal displacement and the elevation, respectively. Both x and y are modeled as independent Gaussian random variables with different jitters for the horizontal displacement (σ_x) and the elevation (σ_y), and different boresight errors in each axis of the receiver plane (μ_x and μ_y) i.e., $x \sim N(\mu_x, \sigma_x)$ and $y \sim N(\mu_y, \sigma_y)$. It must be noted that a circular detection aperture of radius a is assumed at the receiver, shown in Fig. 1, where the beam footprint with generalized misalignment on the detector plane is illustrated. Furthermore, the approximation in Eq. (6) is in good agreement with the exact value when the beam width $\omega_z > 6a$, as shown in [17, appendix]. The approximate expression for h_p can even be used when $\omega_z < 6a$ but obtaining a normalized mean-squared error (NMSE) NMSE $> 10^{-3}$. Therefore, $\varphi_x = \omega_{z_{eq}}/2\sigma_x$ and $\varphi_y = \omega_{z_{eq}}/2\sigma_y$ are the ratios between the equivalent beam radius at the receiver and the corresponding pointing error displacement standard deviation (jitter) at the receiver. The radial displacement at the receiver is distributed according to the well-known Beckmann distribution, whose integral-form PDF can be found in [21, eqn. (2.37)] as follows

$$f_r(r) = \frac{r}{2\pi\sigma_x\sigma_y} \times \int_0^{2\pi} \exp\left(-\frac{(r\cos\theta-\mu_x)^2}{2\sigma_x^2} - \frac{(r\sin\theta-\mu_y)^2}{2\sigma_y^2}\right) d\theta. \tag{7}$$

This is a versatile statistical model that includes many distributions as special cases such as Rayleigh, Hoyt and lognormal-Rician, among others [17]–[19]. In order to efficiently find asymptotic closed-form solutions for the outage performance, an MGF-based approach is used here due to the fact that the Beckmann distribution is mathematically intractable. The MGF corresponding to the squared Beckmann distribution (r^2) can easily be derived from the sum of two independent squared normal random variates as

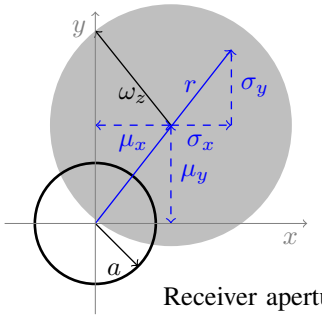

Fig. 1: Beam footprint with pointing errors on the receiver.

$$M_{r^2}(t) = \mathbb{E}[e^{t\cdot r^2}] = \frac{\exp\left(\frac{\mu_x^2 t}{1-2t\sigma_x^2} + \frac{\mu_y^2 t}{1-2t\sigma_y^2}\right)}{\sqrt{\left(1-2t\sigma_x^2\right)\left(1-2t\sigma_y^2\right)}}, \tag{8}$$

with $\mathbb{E}[\cdot]$ denoting expectation.

IV. Asymptotic Outage Performance Analysis

The outage probability (OP), P_{out}, can be defined as the probability that the instantaneous combined SNR, γ_T, falls below a certain specified threshold, γ_{th}, that is

$$P_{\text{out}} := P(\gamma_T \le \gamma_{th}) = \int_0^{\gamma_{th}} f_{\gamma_T}(h)dh. \tag{9}$$

Using Eq. (9), the outage probability can be written as

$$P_{\text{out}} = P(4\gamma h^2 \le \gamma_{th}) = \int_0^{\sqrt{\gamma_{th}/4\gamma}} f_h(h)dh. \tag{10}$$

The PDF of $h = L \cdot h_a \cdot h_p$ can be written as

$$f_h(h) = \int_0^{A_0} f_{h|h_p}(h|L\cdot h_p) f_{h_p}(h_p)dh_p, \tag{11}$$

where $f_{h|h_p}(h|L\cdot h_p)$ is the conditional probability given a pointing error state h_p and L acts as a scaling factor. Hence, the resulting conditional distribution can be written as

$$f_{h|h_p}(h|L\cdot h_p) = \frac{1}{L\cdot h_p} f_{h_a}\left(\frac{h}{L\cdot h_p}\right). \tag{12}$$

Determining the combined effect of the EW atmospheric turbulence and generalized pointing errors might be mathematically intractable due to the fact that the Beckmann distribution presents certain impediments from a practical point of view since a closed-form solution for its integral in Eq. (7) is unknown. As a result, the asymptotic behavior at high SNR is investigated here in order to carefully study how generalized pointing errors and atmospheric turbulence impact on outage performance. In this way, an asymptotic expression for the atmospheric turbulence is adopted in order to obtain simple closed-form expressions, assuming a single polynomial term as follows

$$f_{h_a}(h_a) \doteq m_1 h_a^{m_2-1}, \quad h_a \ge 0 \tag{13}$$

based on the fact that that the asymptotic behavior of the performance of FSO communication systems is dominated by the

behavior of the PDF near the origin, i.e., $f_{h_a}(h_a)$ at $h_a \to 0^+$ determines high SNR performance [24]. The parameter m_1 is a positive constant, and the parameter m_2 quantifies the order of smoothness of $f_{h_a}(h_a)$ at the origin. Both parameters are determined by the channel PDF in Eq. (2). The high SNR approximations are especially useful for performance analysis of FSO systems, where severe fading renders necessary a large SNR for achieving a target OP. Hence, as shown in the Appendix, an asymptotic expression of $f_{h_a}(h_a)$ can be obtained from as follows

$$f_{h_a}(h_a) \doteq m_1 h_a^{m_2-1} = \frac{\alpha\beta}{\eta^{\alpha\beta}} h_a^{\alpha\beta-1}, \quad h_a \geq 0. \tag{14}$$

Therefore, substituting Eq. (14) into Eq. (12) gives

$$\begin{aligned} f_{h|h_p}(h|L\cdot h_p) =& \frac{1}{L\cdot h_p} f_{h_a}\left(\frac{h}{L\cdot h_p}\right) \\ &\doteq \frac{\alpha\beta}{L\eta^{\alpha\beta}} \frac{1}{h_p}\left(\frac{h}{L\cdot h_p}\right)^{\alpha\beta-1}. \end{aligned} \tag{15}$$

The asymptotic behavior corresponding to the PDF of h can be expressed as follows

$$f_h(h) \doteq \frac{\alpha\beta}{L\eta^{\alpha\beta}} \int_0^{A_0} \frac{1}{h_p}\left(\frac{h}{L\cdot h_p}\right)^{\alpha\beta-1} f_{h_p}(h_p) dh_p. \tag{16}$$

After some straightforward algebraic manipulations in Eq. (16), we can express the PDF of h as

$$f_h(h) \doteq \frac{\alpha\beta}{(L\eta)^{\alpha\beta}} h^{\alpha\beta-1} \int_0^{A_0} h_p^{-\alpha\beta} f_{h_p}(h_p) dh_p. \tag{17}$$

In order to avoid computing the PDF corresponding to the generalized pointing error, $f_{h_p}(h_p)$, we use an MGF-based approach. Equivalently, notice that $h_p(r;z) \approx A_0 \exp\left(\frac{-2r^2}{\omega_{z_{eq}}^2}\right)$, we can rewrite the expression in Eq. (17) as follows

$$f_h(h) \doteq \frac{\alpha\beta h^{\alpha\beta-1}}{(L\eta A_0)^{\alpha\beta}} \int_0^{\infty} \exp\left(\frac{\alpha\beta r^2}{\omega_{z_{eq}}^2}\right) f_{r^2}(r^2) dr^2. \tag{18}$$

Notice that the MGF of a random variable χ can also be interpreted as the expectation of the random variable $\exp(t\chi)$, the integral in Eq. (18) can easily be computed as the MGF corresponding to the random variable r^2 as

$$\begin{aligned} f_h(h) \doteq& \frac{\alpha\beta h^{\alpha\beta-1}}{(L\eta)^{\alpha\beta} A_0^{\alpha\beta}} \mathbb{E}\left[e^{\frac{2\alpha\beta r^2}{\omega_{z_{eq}}^2}}\right] \\ =& \frac{\alpha\beta M_{r^2}\left(\frac{2\alpha\beta}{\omega_{z_{eq}}^2}\right)}{(L\eta A_0)^{\alpha\beta}} h^{\alpha\beta-1}, \end{aligned} \tag{19}$$

where $\omega_{z_{eq}}^2 = 4\sigma_x\sigma_y\varphi_x\varphi_y$. With the expression in Eq. (19), the closed-form asymptotic solution for the outage probability corresponding to the considered SISO FSO link with generalized pointing errors can readily be obtained as

$$P_{\text{out}} \doteq \frac{M_{r^2}\left(\frac{\alpha\beta}{2\sigma_x\sigma_y\varphi_x\varphi_y}\right)}{(2L\eta A_0)^{\alpha\beta}} \left(\frac{\gamma_{th}}{\gamma}\right)^{\alpha\beta/2}, \tag{20}$$

where $M_{r^2}(\cdot)$ is expressed as follows

$$\begin{aligned} &M_{r^2}\left(\frac{\alpha\beta}{2\sigma_x\sigma_y\varphi_x\varphi_y}\right) \\ &= \frac{\varphi_x\varphi_y \exp\left(\frac{\alpha\beta\mu_x^2}{2\sigma_x^2(\varphi_x^2-\alpha\beta)} + \frac{\alpha\beta\mu_y^2}{2\sigma_y^2(\varphi_y^2-\alpha\beta)}\right)}{\sqrt{(\varphi_x^2-\alpha\beta)(\varphi_y^2-\alpha\beta)}}. \end{aligned} \tag{21}$$

The $M_{r^2}(\cdot)$ must always be greater than 0. It is straightforward to show that the outage probability behaves asymptotically as $(O_c\gamma)^{-O_d}$, where O_d and O_c denote outage diversity and coding gain, respectively [24]. At high SNR, the outage diversity determines the slope of the outage probability versus average SNR curve in a log-log scale and the coding gain (in decibels) determines the shift of the curve in SNR. It must be noted that the outage diversity is $O_d = \alpha\beta/2$ when the effect of the EW atmospheric turbulence is the dominant effect in relation to generalized pointing errors at high SNR, i.e, when $\alpha\beta < \{\varphi_x^2, \varphi_y^2\}$ according to Eq. (21) and, hence, the asymptotic expression derived in Eq. (20) only holds when the atmospheric turbulence is the dominant effect. In other words, the outage diversity only depends on the atmospheric turbulence when larger amounts of generalized misalignment are not assumed. When pointing errors dominate, it is conjectured that outage diversity will depend on φ_x^2, φ_y^2 and nonzero boresight errors, however, this case is difficult to derive given the Beckmann distribution. It can be shown that most practical terrestrial FSO systems operate under the condition of atmospheric turbulence is the dominant effect. This will be verified numerically in Section V. It must also be mentioned that a much higher outage diversity can be achieved under this condition and, hence, a much better performance is obtained. As a result, the adoption of the transmitter with accurate control of their beam width is especially important here to satisfy this desired FSO scenario in order to maximize the outage diversity.

It can be convenient to compare with the outage performance obtained here in a similar context without considering generalized pointing errors. Notice that the impact of pointing errors in our analysis can be suppressed by assuming $A_0 \to 1$, $\mu_x = \mu_y = 0$, $\varphi_x^2 \to \infty$ and $\varphi_y^2 \to \infty$, the corresponding asymptotic expression can easily be derived from Eq. (20) as follows

$$P_{\text{out}}^{npe} \doteq \frac{1}{(2L\eta)^{\alpha\beta}} \left(\frac{\gamma_{th}}{\gamma}\right)^{\alpha\beta/2}. \tag{22}$$

Note that the above expression is the asymptotic behavior corresponding to the outage probability over EW atmospheric turbulence when no generalized pointing errors are considered, which allows us to easily obtain once again the outage diversity, i.e., the slope of the outage probability versus SNR. It is noteworthy to mention that the outage diversity, $O_d = \alpha\beta/2$, corresponding to the EW atmospheric turbulence had not been derived in any earlier work [8], [9], [11]–[14], [16], which not only depends on channel parameters but also on AA.

V. Numerical Results and Discussion

As an illustration of the asymptotic outage probability expression obtained in Eq. (20), some numerical results over EW

atmospheric turbulence channels with generalized pointing errors are carefully analyzed in this section. It must be noted that the system configuration adopted in this study is used in most practical terrestrial FSO communication systems as in [17], [19], [25], [26], shown in Table I. Different weather conditions are adopted in this paper: haze visibility of 4 km with $C_n^2 = 2 \times 10^{-14}\ m^{-2/3}$ and clear visibility of 16 km with $C_n^2 = 8 \times 10^{-14}\ m^{-2/3}$, corresponding to moderate and strong turbulence conditions, respectively. A wavelength value of $\lambda = 1550$ nm is chosen due to its low attenuation as well as the proliferation of high-quality transmitter and detector components. A source-destination link distance of $d_{SD} = 3$ km is assumed together with a $D = 10$ cm receiver aperture in order to study a practical FSO communications system, wherein the typical link distance values are between 1-5 km as well as typical values for the receiver diameter are on the order of 5-20 cm. Rytov variance values of $\sigma_R^2 = \{3, 12\}$ are derived for $d_{SD} = 3$ km corresponding to moderate and strong turbulence, respectively. Additionally, the optical beam width is relatively wide, 2-10 mrad of divergence at $1/e^2$ that is equivalent to a beam spread of 6-30 m at 3 km (the source-destination link distance considered here). Nevertheless, a narrower beam width should be used to avoid a high geometric loss when link distances greater than one kilometer are assumed. In this case, the use of automatic pointing and tracking systems is required in order to reduce pointing error effects, typically between 0.05-1 mrad of divergence at $1/e^2$ that is equivalent to a beam spread of 15-300 cm at 3 km [25], [26]. Pointing errors are present here assuming different jitters values and nonzero boresight errors, which can take values up to 0.1 mrad or even much smaller [27]. Parameters α, β and η are calculated from Eq. (3), obtaining values of $(\alpha, \beta, \eta) = (4.57, 1.18, 0.52)$ and $(\alpha, \beta, \eta) = (4.31, 1.35, 0.58)$ corresponding to moderate and strong turbulence, respectively, for a source-destination link distance of $d_{SD} = 3$ km and a 10 cm receiver aperture.

TABLE I: An Example of a FSO System Configuration.

Parameter	Symbol	Value
source-destination link distance	d_{SD}	3 km
Wavelength	λ	1550 nm
Receiver aperture diameter	$D = 2a$	10 cm
Transmit divergence at $1/e^2$	θ_z	0.66 mrad
Beam width at 3 km	ω_z	≈200 cm
Jitter angle at $1/e^2$	θ_s	0.11 mrad
Maximum jitter at 3 km	σ_x, σ_y	≈35 cm
Boresight angle at $1/e^2$	θ_b	0.06 mrad
Maximum boresight at 3 km	μ_x, μ_y	≈20 cm

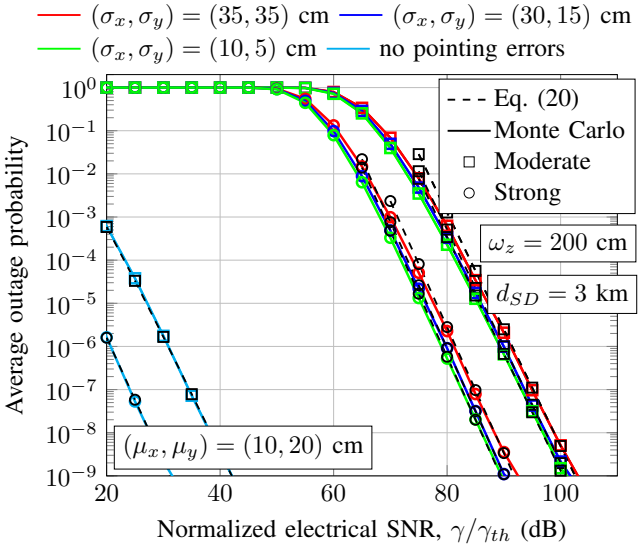

Fig. 2: Outage performance for a 10 cm receiver aperture together with a beam width value of $\omega_z = 200$ cm when different jitter values of $(\sigma_x, \sigma_y) = \{(35, 35), (30, 15), (10, 5)\}$ cm are assumed under different atmospheric turbulence conditions.

A. Outage probability

The results corresponding to this asymptotic outage performance analysis are depicted in Fig. 2 as a function of the inverse normalized threshold SNR, γ/γ_{th}, when a $D = 10$ cm receiver aperture is used. This aperture size has been selected according to the technical specifications for commercial FSO applications given in [28]. A beam width value of $\omega_z = 200$ cm is considered corresponding to a 0.66 mrad of divergence at 3 km, approximately. It can be shown that a value of $\varphi^2 = 6.25$ greater than the product of $\alpha\beta$ is computed when a beam width value of $\omega_z = 200$ cm and a jitter angle of 0.13 mrad at $1/e^2$ that is equivalent to a value jitter of 40 cm at 3 km are assumed. Hence, atmospheric turbulence is the dominant effect even when the greatest jitter value is considered. Note that the condition $\omega_z > 6a$ is satisfied for this aperture size, i.e, $D = 10$ cm. At the same time, different jitters values of $(\sigma_x, \sigma_y) = \{(35, 35), (30, 15), (10, 5)\}$ cm together with boresight error values of $(\mu_x, \mu_y) = (10, 20)$ cm are considered in order to evaluate how generalized pointing errors impact on the FSO communications system under different atmospheric turbulence and aperture averaging conditions. In order to confirm the accuracy and usefulness of the derived expression, Monte Carlo simulation results, where the FSO link is modeled using Eq. (1), and generating the corresponding variates from the exact PDF in Eq. (2) for EW atmospheric turbulence and Eq. (6) for generalized pointing errors are used. Although the typical outage performance target is set to 10^{-6} for most practical FSO systems, Monte Carlo simulation results only up to 10^{-9} (due to long time involved) are included in this analysis due to the fact that targets as low as 10^{-9} are typically aimed to achieve. As can be seen in Fig. 2, the derived expression for the outage probability is in good agreement with these simulation results. Furthermore, simulation results corroborate that the asymptotic expression obtained here lead to a simple bound on the OP that get tighter over a wider range of SNR. Outage performance without pointing errors is also displayed using Eq. (22). As commented before, a higher diversity order, which is determined by the product of $\alpha\beta/2$, is achieved when the atmospheric turbulence is the dominant effect in relation

to generalized pointing errors. This assumption is widely adopted in most practical terrestrial FSO communication systems. Further, it can be observed that the outage probability decreases as generalized pointing errors increase. In other words, jitters values of $(\sigma_x, \sigma_y) = \{(35, 35), (30, 15)\}$ cm significantly reduce much more the outage performance than jitters values of $(\sigma_x, \sigma_y) = (10, 5)$ cm in both atmospheric turbulence scenarios. It should be highlighted that the 10 cm receiver aperture is considered as a aperture-averaged receiver under moderate-to-strong turbulence due to the fact that this diameter is greater than the atmospheric coherence length $\rho_0 = \{12.6, 5.5\}$ mm under moderate and strong turbulence, respectively. As expected, aperture averaging can significantly improve the performance under moderate and strong atmospheric turbulence regardless of generalized pointing errors. Note that atmospheric turbulence is much more damaging for moderate turbulence than strong turbulence conditions. This phenomenon has been investigated by different authors in the literature [23], [29], where pointing error effects were not considered. On the one hand, outage diversities of $O_d = 2.7$ and $O_d = 2.92$ are obtained over moderate and strong turbulence, respectively. On the other hand, a coding gain of 8.3 dB is achieved over strong turbulence channels in relation to moderate turbulence channels when a different visibility is considered. Although, a coding gain of approximately 1 dB is also achieved over strong turbulence when the same visibility is assumed for both turbulence regimes. It can also be observed that aperture averaging can take place even for relatively small apertures, i.e. $D = 10$ cm, particularly under strong turbulence conditions, as commented on [23].

B. Impact of generalized pointing errors

Taking into account the coding gain O_c in Eq. (20), the impact of generalized pointing errors translates into a loss, $Loss_{pe}[dB]$, relative to EW atmospheric turbulence without generalized misalignment fading in Eq. (22) given by

$$Loss_{pe}[dB] \triangleq \frac{20}{\alpha\beta} \log_{10}\left(A_0^{-\alpha\beta} M_{r^2}\left(\frac{\alpha\beta}{2\sigma_x\sigma_y\varphi_x\varphi_y}\right)\right). \quad (23)$$

The above expression computes the additional power needed to obtain a given outage performance when there is pointing error versus no pointing error. The loss, $Loss_{pe}$[dB], derived above is plotted in Fig. 3 for a 10 cm receiver aperture as a function of the source-destination link distance when different jitter values and boresight errors are considered as well as different turbulence conditions. It can be observed in Fig. 3 that the loss generally remains at a constant level as source-destination link distance increases. However, it can also be seen in Fig. 3(b) that the loss slightly increases as source-destination links distance increases under strong turbulence conditions due to the fact that the product of $\alpha\beta$ increases as source-destination link distance increases for this aperture size ($D = 10$ cm) under strong turbulence. Additionally, the loss increases considerably as nonzero boresight errors increase, i.e., as the severity of pointing errors is getting great.

In order to minimize the effect of generalized pointing errors, the beam width, ω_z, is chosen to minimize the outage

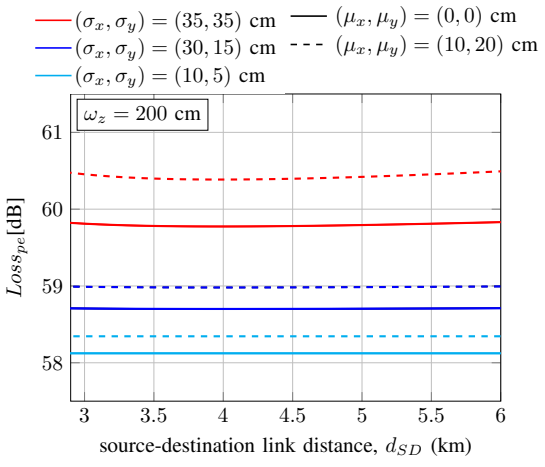

(a) Moderate turbulence.

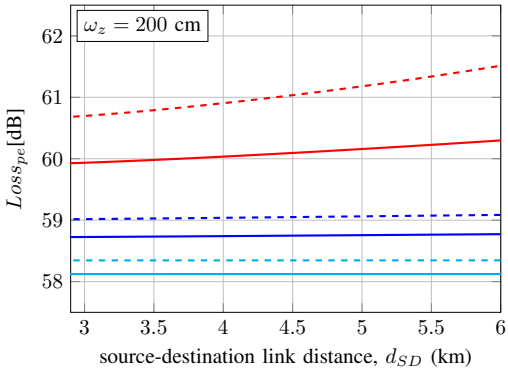

(b) Strong turbulence.

Fig. 3: Loss, $Loss_{pe}$[dB], for (a) moderate atmospheric turbulence, and (b) strong atmospheric turbulence when a 10 cm receiver aperture is considered under different nonzero boresight error values.

probability given in Eq. (20) in Fig. 4. Note that the beam width is an important parameter to consider in the FSO communications link design. In this way, the optimization procedure is finished by finding the optimum beam width, $\omega_{z_{opt}}$, that gives the minimum loss in Eq. (23). This optimum beam width is achieved by using numerical observation methods for different jitters values and an aperture size of $D = 10$ cm. The optimum value is obtained with the help of software packages such as Mathematica (version 10.4.1.0) by using a derivative-based method, which was found through a sweep of the beam width subject to constraints such as $\omega_z > 6a$, $\omega_z > \{\sigma_x, \sigma_y\}$ and $\alpha\beta < \{\varphi_x^2, \varphi_y^2\}$. It can be seen in Fig. 4 that numerical results for the optimum beam width are plotted as a function of the horizontal jitter when different vertical jitter values of $\sigma_y = \{10, 20, 25, 30\}$ cm are assumed. From this figure, it can be deduced that the outage performance optimization provides numerical results (red, blue, green and cyan colors) tending to a linear performance for each value of σ_y (black color), where the corresponding slope only depends on the EW atmospheric turbulence. Note that the optimum beam width depends on the maximum value between σ_x and σ_y. This linear behavior leads to easily obtain a first-degree

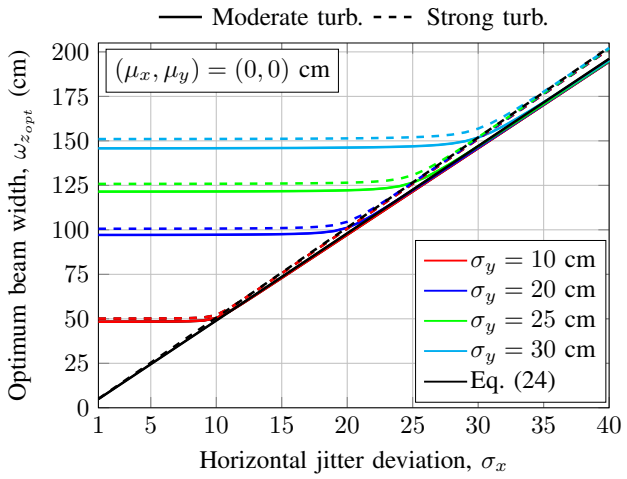

Fig. 4: Optimum beam width, $\omega_{z_{opt}}$, versus horizontal jitter, σ_x, when different vertical jitter values, σ_y, are assumed in FSO links over EW atmospheric turbulence together with a source-destination link distance of $d_{SD} = 3$ km for a 10 cm receiver aperture.

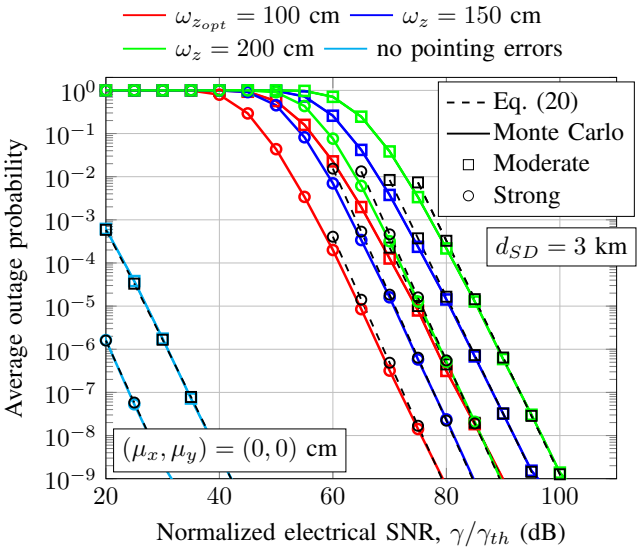

Fig. 5: Outage performance for a 10 cm receiver aperture together with jitter values of $(\sigma_x, \sigma_y) = (5, 20)$ cm when different beam width values of $\omega_z = \{100, 150, 200\}$ cm are assumed under different atmospheric turbulence conditions.

polynomial, which is derived from the obtained optimum beam width values through polynomial interpolation given by

$$\omega_{z_{opt}} \approx (-0.036(\alpha\beta)^2 + 0.77\alpha\beta + 1.76)\sigma_x, \qquad (24)$$

where the slope follows a quadratic form in $\alpha\beta$. In the light of the expression obtained in Eq. (24), it can be observed that the optimum beam width is strongly dependent on the outage diversity, $O_d = \alpha\beta/2$. In other words, this optimum beam width depends on the aperture averaging as well as on the receiver aperture diameter due to the fact that α and β are related to these parameters through the scintillation index as can be seen in Eqs. (3) and (5). As can be seen in Fig. 4, it is clearly depicted that the approximation remains very close to numerical results. Interestingly, it can also be seen in this figure that different slopes are derived for the optimum beam width when the product of $\alpha\beta$ is equal to 5.41 and 5.84 for moderate and strong turbulence, respectively. It is noteworthy to mention that a slightly greater optimum beam width is required for strong turbulence in comparison with moderate turbulence due to the fact that the product of $\alpha\beta$ is greater under strong turbulence than moderate turbulence. It should be noted that the above expression can be used to estimate the optimum beam width when the boresight error takes small values up to 0.03 mrad, as reported in [27].

Numerical results for the optimum beam width are used in Fig. 5 for a 10 cm receiver aperture when jitter values of $(\sigma_x, \sigma_y) = (5, 20)$ cm are assumed under different turbulence conditions. According to the expression in Eq. (23), it can be observed in Fig. 5 that losses of 48, 53.2 and 57.2 decibels are achieved for beam width values of $\omega_z = \{100, 150, 200\}$ cm under moderate turbulence conditions. Analogously, losses of 48, 53.2 and 57.2 decibels are also achieved for beam width values of $\omega_z = \{100, 150, 200\}$ cm under strong turbulence conditions. Note that the minimum achievable loss for jitter values of $(\sigma_x, \sigma_y) = (5, 20)$ cm is 48 dB for an optimum beam width of $\omega_{z_{opt}} = 100$ cm in this case.

C. Impact of different jitters for the elevation and the horizontal displacement and nonzero boresight errors

For a better understanding of the impact of assuming different jitters for the elevation and the horizontal displacement, the loss, $Loss_{pe}$[dB] in Eq. (23), is plotted in Fig. 6 for a 10 cm receiver aperture as a function of the relation between σ_y and σ_x when different boresight error values are considered as well as different turbulence conditions. As can be seen in both subfigures, the effect of different jitters for the elevation and the horizontal displacement has also been evaluated, and, hence, it can be observed that as the relation between jitters increases, the outage performance decreases.

Finally, the impact of nonzero boresight pointing errors translates into a loss, $Loss_{nzb}[dB]$, relative to zero boresight pointing errors that can be deduced as

$$Loss_{nzb}[dB] \triangleq \frac{(10/\ln(10))\mu_x^2}{\sigma_x\left(\sigma_y\varphi_x\varphi_y - \alpha\beta\sigma_x\right)} + \frac{(10/\ln(10))\mu_y^2}{\sigma_y\left(\sigma_x\varphi_x\varphi_y - \alpha\beta\sigma_y\right)}. \qquad (25)$$

For the sake of clarity, the above expression computes the loss of nonzero boresight errors versus zero boresight errors for different jitter values. In the light of the above expression, it must be noted that the impact of nonzero boresight error is symmetric in relation to the y-axis. The impact of nonzero boresight error, $Loss_{nzb}$[dB], is also studied in Fig. 7 for a 10 cm receiver aperture as a function of the horizontal boresight error when different vertical boresight error values are assumed as well as different turbulence conditions. As expected, the effect of nonzero boresight error can dramatically reduce the performance of FSO communication systems, increasing

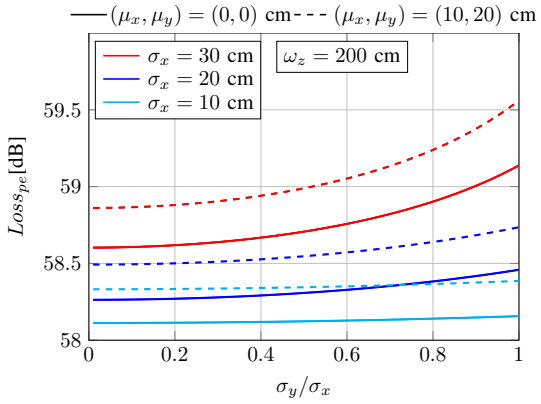

(a) Moderate turbulence.

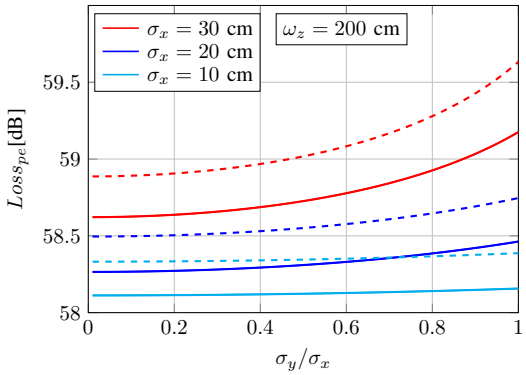

(b) Strong turbulence.

Fig. 6: Loss, $Loss_{pe}$[dB], for (a) moderate atmospheric turbulence, and (b) strong atmospheric turbulence when a 10 cm receiver aperture is considered under different nonzero boresight error values.

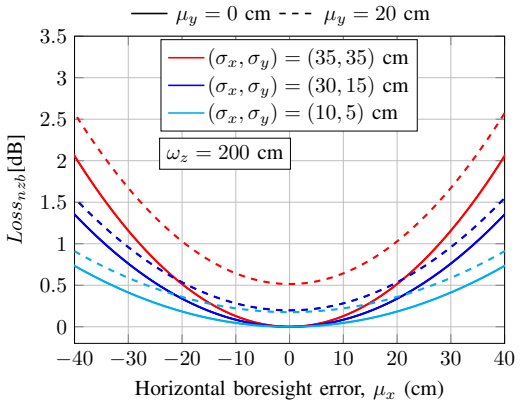

(a) Moderate turbulence.

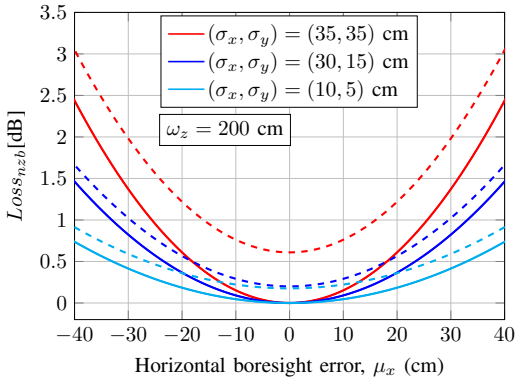

(b) Strong turbulence.

Fig. 7: Loss, $Loss_{nzb}$[dB], for (a) moderate atmospheric turbulence, and (b) strong atmospheric turbulence when a 10 cm receiver aperture is considered under different nonzero boresight error values.

its effect as jitter values increase. Equivalently, the same results and conclusions can be drawn when the impact of nonzero boresight is depicted as a function of the vertical boresight error instead of the horizontal boresight error.

Apparently, taking into account obtained results, we can say that the impact of generalized pointing errors is approximately the same over moderate and strong turbulence conditions when an aperture-averaged receiver is considered. However, it is important emphasize from these figures that moderate turbulence might be slightly more robust than strong turbulence when larger amounts of misalignment in terms of jitter variances are assumed. It should be highlighted from these figures that the effect of different jitters is more damaging than the effect of nonzero boresight errors in terrestrial FSO links due to the fact that the maximum nonzero boresight error reported is much smaller than jitter variances. Moreover, the effect of nonzero boresight error is strongly related to jitter values since its effect increases as jitter variances also increase.

VI. Conclusion

A study of the outage probability of FSO communication links over EW and generalized misalignment fading channels is performed in order to readily study how basic system parameters impact on the FSO communications system, wherein the radial displacement at the receiver is determined by a Beckmann distribution. This statistical distribution allows us to take into account not only the effect of different jitters for the elevation and the horizontal displacement but also the simultaneous effect of different boresight errors for each axis.

From this analysis, we can conclude that the beam width can be optimized in order to improve the outage performance of FSO links in presence of both EW atmospheric turbulence and generalized pointing errors. It can also be concluded that the optimum beam width is a feasible method for reducing pointing error losses in terrestrial FSO links. This latter is due to the fact that the optimum beam width not only depends on the outage diversity but also on the aperture averaging, obtaining different values for moderate and strong turbulence conditions.

Additionally, it is concluded that aperture averaging can take place even for relatively small apertures, particularly under strong turbulence conditions. Also, it has been demonstrated that the aperture averaging has a strong effect on both outage diversity and coding gain. Obtained results corroborate that both moderate and strong turbulence channels are almost equally affected by generalized pointing errors when an aperture-averaged receiver is considered, being the effect of

different jitters more damaging than the effect of nonzero boresight errors in most practical FSO links. In this way, strong turbulence channels might be more interesting than moderate turbulence channels as a consequence of achieving not only a greater coding gain but also a higher outage diversity under aperture averaging conditions. Finally, the study can be extended to other atmospheric statistical models, which can be expanded into a Maclaurin series.

APPENDIX
ASYMPTOTIC BEHAVIOR OF EW ATMOSPHERIC TURBULENCE

When the PDF of the atmospheric turbulence can be expanded in a Maclaurin series, the exact outage probability can be expressed as a power series. In this case, the first term of this series is the dominant term, i.e., $OP \doteq (O_c\gamma)^{-O_d}$. Hence, the corresponding asymptotic expression of $f_{h_a}(h_a)$ can easily be obtained from the corresponding series expansion of the exponential function in Eq. (2) [31, eqn. (1.211.1)] as follows

$$\begin{aligned} f_{h_a}(h_a) &\doteq \frac{\alpha\beta}{\eta}\left(\frac{h_a}{\eta}\right)^{\beta-1}\left\{1-1+\frac{h_a^{\beta}}{\eta^{\beta}}\right\}^{\alpha-1} \\ &\doteq \frac{\alpha\beta}{\eta}\left(\frac{h_a}{\eta}\right)^{\beta-1}\frac{h_a^{\alpha\beta-\beta}}{\eta^{\alpha\beta-\beta}} \doteq \frac{\alpha\beta}{\eta^{\alpha\beta}}h_a^{\alpha\beta-1}. \end{aligned} \tag{26}$$

ACKNOWLEDGMENT

This work was partially performed at McMaster University during a research fellowship of the first author. The authors would like to acknowledge the received support from the free-space optical communications algorithms laboratory (FOCAL) at this university. The authors are also grateful for financial support from the Universidad de Málaga (UMA) and the Junta de Andalucía (research group "Communications Engineering (TIC-0102)").

REFERENCES

[1] M. A. Khalighi and M. Uysal, "Survey on free space optical communication: A communication theory perspective," *Communications Surveys & Tutorials, IEEE*, vol. 16, no. 4, pp. 2231–2258, 2014.

[2] L. C. Andrews and R. L. Phillips, *Laser beam propagation through random media*. SPIE press Bellingham, WA, 2005, vol. 1.

[3] S. D. Lyke, D. G. Voelz, and M. C. Roggemann, "Probability density of aperture-averaged irradiance fluctuations for long range free space optical communication links," *Appl. Opt.*, vol. 48, no. 33, pp. 6511–6527, Nov 2009.

[4] R. Barrios and F. Dios, "Exponentiated Weibull distribution family under aperture averaging for Gaussian beam waves," *Opt. Express*, vol. 20, no. 12, pp. 13 055–13 064, 2012.

[5] ——, "Exponentiated Weibull model for the irradiance probability density function of a laser beam propagating through atmospheric turbulence," *Optics & Laser Technology*, vol. 45, pp. 13–20, 2013.

[6] H. Yura and T. Rose, "Exponentiated Weibull distribution family under aperture averaging Gaussian beam waves: comment," *Opt. Express*, vol. 20, no. 18, pp. 20 680–20 683, 2012.

[7] R. Barrios and F. Dios, "Reply to comment on "The Exponentiated Weibull distribution family under aperture averaging for Gaussian beam waves"," *Opt. Express*, vol. 20, no. 18, pp. 20 684–20 687, 2012.

[8] X. Yi, Z. Liu, and P. Yue, "Average BER of free-space optical systems in turbulent atmosphere with Exponentiated Weibull distribution," *Opt. Letters*, vol. 37, no. 24, pp. 5142–5144, 2012.

[9] P. Wang, L. Zhang, L. Guo, F. Huang, T. Shang, R. Wang, and Y. Yang, "Average BER of Subcarrier intensity modulated free-space optical systems over the Exponentiated Weibull fading channels," *Opt. Express*, vol. 22, no. 17, pp. 20 828–20 841, 2014.

[10] M. Cheng, Y. Zhang, J. Gao, F. Wang, and F. Zhao, "Average capacity for optical wireless communication systems over Exponentiated Weibull distribution non-kolmogorov turbulent channels," *Applied Optics*, vol. 53, no. 18, pp. 4011–4017, 2014.

[11] P. Wang, T. Cao, L. Guo, R. Wang, and Y. Yang, "Performance analysis of multihop parallel free-space optical systems over Exponentiated Weibull fading channels," *Photonics Journal, IEEE*, vol. 7, no. 1, pp. 1–17, Feb 2015.

[12] P. Sharma, A. Bansal, P. Garg, T. Tsiftsis, and R. Barrios, "Performance of FSO links under Exponentiated Weibull turbulence fading with misalignment errors," in *Communications (ICC), 2015 IEEE International Conference on*. IEEE, 2015, pp. 5110–5114.

[13] P. Wang, J. Zhang, L. Guo, T. Shang, T. Cao, R. Wang, and Y. Yang, "Performance analysis for relay-aided multihop BPPM FSO communication system over Exponentiated Weibull fading channels with pointing error impairments," *Photonics Journal, IEEE*, vol. 7, no. 4, pp. 1–20, Aug 2015.

[14] X. Yi and M. Yao, "Free-space communications over Exponentiated Weibull turbulence channels with nonzero boresight pointing errors," *Opt. Express*, vol. 23, no. 3, pp. 2904–2917, 2015.

[15] R. Boluda-Ruiz, A. García-Zambrana, B. Castillo-Vázquez, and C. Castillo-Vázquez, "Impact of nonzero boresight pointing error on ergodic capacity of MIMO FSO communication systems," *Opt. Express*, vol. 24, no. 4, pp. 3513–3534, Feb 2016.

[16] P. Wang, J. Qin, L. Guo, and Y. Yang, "BER performance of FSO limited by shot and thermal noise over Exponentiated Weibull fading channels," *Photonics Technology Letters, IEEE*, vol. 28, no. 3, pp. 252–255, 2016.

[17] A. A. Farid and S. Hranilovic, "Outage capacity optimization for free-space optical links with pointing errors," *J. Lightwave Technol., IEEE/OSA*, vol. 25, no. 7, pp. 1702–1710, July 2007.

[18] W. Gappmair, S. Hranilovic, and E. Leitgeb, "OOK performance for terrestrial FSO links in turbulent atmosphere with pointing errors modeled by Hoyt distributions," *Commun. Letters, IEEE*, vol. 15, no. 8, pp. 875–877, 2011.

[19] F. Yang, J. Cheng, and T. Tsiftsis, "Free-space optical communication with nonzero boresight pointing errors," *Commun., IEEE Transactions on*, vol. 62, no. 2, pp. 713–725, 2014.

[20] H. AlQuwaiee, H. C. Yang, and M. Alouini, "On the asymptotic capacity of dual-aperture FSO systems with a generalized pointing error model," *Wireless Commun., IEEE Transactions on*, vol. PP, no. 99, pp. 1–1, 2016.

[21] M. K. Simon and M.-S. Alouini, *Digital communications over fading channels*, 2nd ed. New Jersey: Wiley-IEEE Press, 2005.

[22] I. I. Kim, B. McArthur, and E. J. Korevaar, "Comparison of laser beam propagation at 785 nm and 1550 nm in fog and haze for optical wireless communications," in *Information Technologies 2000*. International Society for Optics and Photonics, 2001, pp. 26–37.

[23] L. C. Andrews, R. L. Phillips, and C. Y. Hopen, "Aperture averaging of optical scintillations: power fluctuations and the temporal spectrum," *Waves in Random Media*, vol. 10, no. 1, pp. 53–70, 2000.

[24] Z. Wang and G. B. Giannakis, "A simple and general parameterization quantifying performance in fading channels," *Commun., IEEE Transactions on*, vol. 51, no. 8, pp. 1389–1398, 2003.

[25] I. I. Kim, R. Stieger, J. A. Koontz, C. Moursund, M. Barclay, P. Adhikari, J. Schuster, E. Korevaar, R. Ruigrok, and C. DeCusatis, "Wireless optical transmission of fast Ethernet, FSSI, STM, and Escon protocol data using the terralink laser communication system," *Optical Engineering*, vol. 37, no. 12, pp. 3143–3155, 1998.

[26] S. Bloom, E. Korevaar, J. Schuster, and H. Willebrand, "Understanding the performance of free-space optics [invited]," *Journal of optical Networking*, vol. 2, no. 6, pp. 178–200, 2003.

[27] D. K. Borah and D. G. Voelz, "Pointing error effects on free-space optical communication links in the presence of atmospheric turbulence," *J. Lightwave Technol., IEEE/OSA*, vol. 27, no. 18, pp. 3965–3973, 2009.

[28] The fSONA Networks, Inc. (2011). [Online]. Available:http://www.fsona.com

[29] M.-A. Khalighi, N. Schwartz, N. Aitamer, and S. Bourennane, "Fading reduction by aperture averaging and spatial diversity in optical wireless systems," *J. Opt. Commun. Netw.*, vol. 1, no. 6, pp. 580–593, 2009.

[30] F. S. Vetelino, C. Young, L. Andrews, and J. Recolons, "Aperture averaging effects on the probability density of irradiance fluctuations in moderate-to-strong turbulence," *Appl. Opt.*, vol. 46, no. 11, pp. 2099–2108, 2007.

[31] I. S. Gradshteyn and I. M. Ryzhik, *Table of integrals, series and products*, 7th ed. Academic Press Inc., 2007.